JACC Vol. 24, No. 1
July 1994:216–24

A New Approach for the Quantification of Complex Lesion Morphology: The Gradient Field Transform; Basic Principles and Validation Results

PIETER M. J. VAN DER ZWET, MSc, JOHAN H. C. REIBER, PhD

Leiden, The Netherlands

Objectives. **This report describes the basic principles and the results from clinical evaluation studies of a new algorithm that has been designed specifically for the quantification of complex coronary lesions.**

Background. **Currently used edge detection algorithms in quantitative coronary arteriography, such as the minimum cost algorithm, are limited in the precise quantification of complex coronary lesions characterized by abruptly changing shapes of the obstruction.**

Methods. **The new algorithm, the gradient field transform, is not limited in its search directions and incorporates the directional information of the arterial boundaries. To evaluate its accuracy and precision, 11 tubular phantoms (sizes 0.6 to 5.0 mm), were analyzed. Second, angiographic images of 12 copper phantoms with U-shaped obstructions were analyzed by both the gradient field transform and the minimum cost algorithm. Third, 25 coronary artery segments with irregularly shaped obstructions were selected from 19 routinely acquired angiograms.**

Results. **The plexiglass phantom study demonstrated an accuracy and precision of −0.004 and 0.114 mm, respectively. The U-shaped copper phantoms showed that the gradient field transform performed very well for short, severe obstructions, whereas the minimum cost algorithm severely overestimated the minimal lumen diameter. From the coronary angiograms, the intraobserver variability in the minimal lumen diameter was found to be 0.14 mm for the gradient field transform and 0.20 mm for the minimum cost algorithm.**

Conclusions. **The new gradient field transform eliminates the limitations of the currently used edge detection algorithms in quantitative coronary arteriography and is therefore particularly suitable for the quantification of complex coronary artery lesions.**

(J Am Coll Cardiol 1994;24:216–24)

Quantitative coronary arteriography has been widely accepted as the method for the accurate assessment of the morphology of coronary vessels and the location and severity of coronary obstructions (1). The accurate derivation of clinically relevant variables, such as the obstruction diameter, interpolated reference diameter, percent diameter stenosis and plaque area, not only facilitates the objective evaluation of clinical research trials, but has also proved to be useful for the selection of the appropriate recanalization devices (2,3).

Over the years, we have developed analytical software packages for both cinefilm (4) and on-line digital applications (5). The high accuracy and precision of these packages have been established and described elsewhere (1,5). In these packages dynamic programming techniques have been used to accurately detect the arterial boundaries automatically (6,7). This algorithm requires a "pathline" as input, which is a rough approximation of the path of the vessel segment to be analyzed. The minimum cost algorithm resamples the image along scanlines perpendicular to the given pathline. For each resampled point, first- and second-derivative values of the brightness profile along the scanline are calculated; the inverse value of the sum of the first and second derivative is then defined as the cost value of that point. Points with low cost values have a high probability of belonging to the contour to be detected, and those with high cost values have a low probability. By applying dynamic programming techniques, a path within the cost matrix with minimal cost is found. In the final step, these contour positions are transformed back to the original image coordinates.

The minimum cost algorithm has been shown to be fast and robust, but it has a number of limitations. First, only one point per scanline can be selected by the algorithm. This limitation requires each scan line to be more or less perpendicular to the edge of the coronary artery. However, when the coronary artery has irregular boundaries, for example, at a complex lesion, this condition may not be satisfied. In the artificial example of Figure 1, the scanline E runs parallel to the actual edge. The dots represent points on the scanline for which a cost value is calculated. The gray level of each point

From the Laboratory for Clinical and Experimental Image Processing, Department of Diagnostic Radiology, University Hospital Leiden, Leiden, The Netherlands. This work was supported in part by a grant from Philips Medical Systems, Best, The Netherlands.

Manuscript received June 10, 1993; revised manuscript received February 10, 1994, accepted February 17, 1994.

Address for correspondence: Dr. Johan H. C. Reiber, Department of Diagnostic Radiology, University Hospital Leiden, Mailstop 1 C2-S, P.O. Box 9600, 2300 RC Leiden, The Netherlands.

0735-1097/94/$7.00

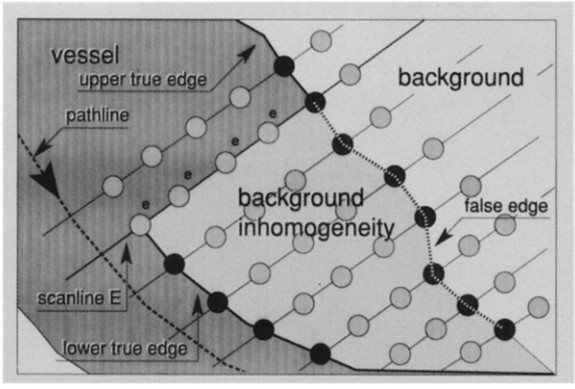

Figure 1. Diagram of a coronary vessel illustrating the limitations of the minimum cost algorithm. Circles represent the individual scanned points; the gray level of each point is a measure of the corresponding cost value. The solid circles have the lowest cost value. Only one point on scanline E will be selected by the minimum cost algorithm, although more points belong to the true edge of the vessel. Moreover, by calculating the edge values only in the direction of the scanlines, the true edge points (e) are assigned high cost values. A false edge, running roughly perpendicular to the scanline will be selected as the vessel boundary. Arrow along the pathline indicates the general direction of search.

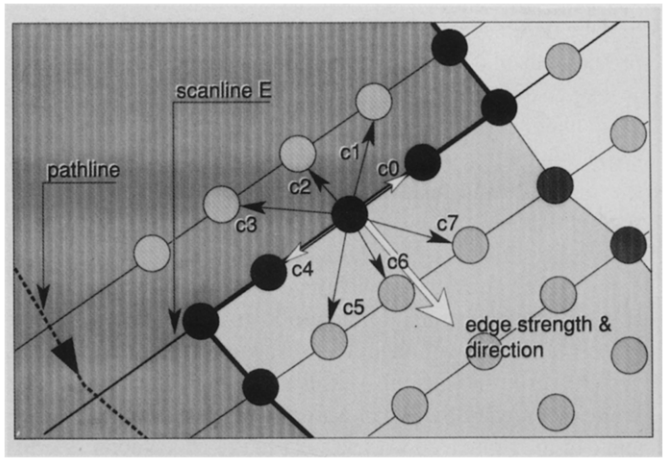

Figure 2. An enlarged detail from Figure 1. By calculating the direction of the edge, different cost values can be assigned to the branches of a node point. In this example, branch c4 will be assigned a low cost value, and branch c0 will be assigned the highest cost value. Branches c1 to c3 and c5 to c7 will be assigned values between these extremes. Arrow along the pathline indicates the general direction of search.

has been chosen such that it represents the corresponding cost value; the dark points have lowest cost values. Under these circumstances, a number of points along the scanline should be included to properly describe the edge. However, with the current minimum cost algorithm, only one of these points will be selected per scanline.

These problems are aggravated by the way the gray values are used in the algorithm. Because the derivatives of the brightness profiles are calculated only along the direction of the scanlines, edge information perpendicular to the scanline (i.e., parallel to the model) is discarded entirely. As a result, the points on scanline E marked "e" are assigned low derivative values and therefore high cost values, even though they are a part of the actual vessel edge. In this case a false edge that is due to background inhomogeneities may have the lowest cost values, thus leading to falsely detected edges. To circumvent these problems and limitations, we developed a new algorithm, the gradient field transform, based on the shortest path algorithm of Dijkstra (8). In this report the basic principles of this algorithm, as well as the results from validation studies based on phantoms and routinely acquired coronary arteriograms, are presented.

Methods

Gradient field transform. The following requirements for this new algorithm for the detection of coronary contours were set: 1) the influence of initial models (e.g., the pathline) should be limited as much as possible; 2) all brightness information available in the image must be used; and 3) its speed must be comparable with the currently used minimum cost algorithm. This improved algorithm is called the gradient field transform because it incorporates the changes in brightness levels for each point in the image (gradients or edge strength values) assessed from all directions. This is in contrast with the conventional minimum cost algorithm, which is based solely on the gradients calculated along the scanlines. In short, scanlines are defined again perpendicular to the pathline, as mentioned earlier for the minimum cost algorithm. As an example, Figure 2 shows a detail of the artificial edge of Figure 1. On each scanline a number of points are defined at equidistant positions. These points define a mathematic graph: a network of nodes and connections between nodes. Each of these "scanpoints" represents a node in the graph. Each scanpoint has directional links or branches (c0 to c7) to all of its eight neighbors. The entire graph consists of a matrix of nodes. The goal of the algorithm now is to find an optimal path between one node on the first scanline of the vessel segment and one node on the last scanline of this segment.

Not only the edge strength, but also the direction of the sum of the first- and second-derivative values in each scanpoint is calculated. Cost values are assigned to each branch in the graph. Each branch from a particular scanpoint to a neighboring scanpoint is assigned a different cost value, which is a function of its edge strength and the angle between the direction of the edge and the direction of the branch. This cost value will be minimal when the angle between the calculated edge vector and the branch direction is +90° and maximal when this angle is −90°.

In Figure 2 the edge vector for the middle point on scanline E is shown. Its length is proportional to the edge strength, whereas its direction is perpendicular to the vessel edge, directed toward the background. Again, on scanline E, multiple points are part of the true vessel edge. Each scanpoint may be connected to each of its neighbors. With the gradient field transform, multiple points on one scanline

JACC Vol. 24, No. 1
July 1994:216–24

may be detected; it is even possible to reverse the search to previous scanlines before continuing with the next scanlines.

For each branch a cost value is calculated (c0 to c7, Fig. 2), depending on the direction of the edge vector (the large arrow emanating from the scan point) and the direction of the branches. In Figure 2 the left contour of the vessel segment should be detected. In this case the contour should always have the vessel at its right-hand side, whatever shape it may have. Thus, the branch labeled c4 will have the lowest cost value because this branch follows the correct direction (characterized by an angle of +90° with respect to the edge vector) while having the vessel at its right-hand side. The branch labeled with c0 will have the highest cost value. The angle of the branch c0 with respect to the edge vector is −90° and it has the vessel at its left-hand side, which is entirely incorrect. The other branches will be assigned cost values in between these two extremes. Note that for the minimum cost algorithm, only the branches labeled c5 to c7 would be allowed, whereas these cost values would be identical and concentrated in the scanpoint.

The shortest path algorithm of Dijkstra (8) allows one to find an optimal path through the graph. Basically, a list of possible paths is maintained while the algorithm traverses through the network. The nodes on the first scanline are defined as *initial nodes*. During each iteration a node is added to the most promising path. For efficiency reasons, the calculation of the relevant branch costs is performed during the corresponding iteration. The algorithm terminates when one of the nodes of the last scanline is added to one of the paths in the list. This means that at the end an optimal path has been found.

In our new analytic software package, the gradient field transform is applied twice. The first time the detected pathline is used as a model, and the positions of the arterial contours are roughly defined by using only a smoothed version of the first-derivative function in the calculation of cost values and only a limited number of points. In the second iteration the initially detected contours are used as models for the accurate detection of the arterial boundaries; at the same time the original image resolution is used. In this iteration correction for the lowpass characteristics of the imaging chain is carried out as well on the basis of the transfer function of the imaging chain. The transfer function has been measured from step phantoms, and an average deconvolution kernel has been defined that effectively eliminates most of the blurring that is apparent in the system. The deconvolution technique deblurres the edges to accurately detect the position of those edges. Without such correction, overestimation of vessel sizes below ~1.2 to 1.3 mm would occur.

An example of a complex lesion (Fig. 3A) with the contours detected with the conventional minimum cost algorithm superimposed is given in Figure 3B, and the results using the gradient field transform are shown in Figure 3C. The improvement in tracking the actual lesional contour is quite evident.

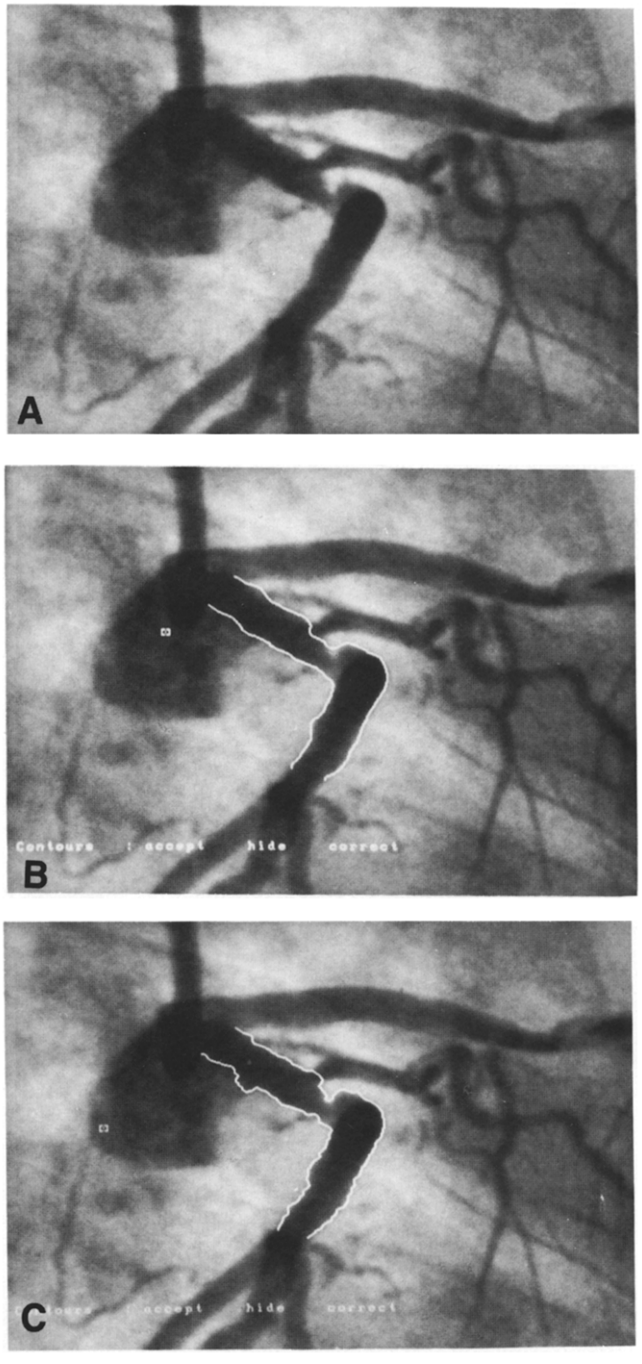

Figure 3. Illustration of the performance of both algorithms on a complex coronary lesion. **A**, Arteriographic image of a coronary obstruction without contours superimposed. **B**, Same coronary artery segment with contours detected by the minimum cost algorithm superimposed. **C**, Contours found by the gradient field transform are superimposed on the same coronary artery segment.

To assess the performance of the gradient field transform, a number of evaluation studies were carried out.

Plexiglass phantom studies. To assess the ultimate accuracy and precision of the gradient field transform under ideal circumstances, digital images of a plexiglass phantom with 11 tubular "vessels," ranging in size from 0.66 to 5.055 mm

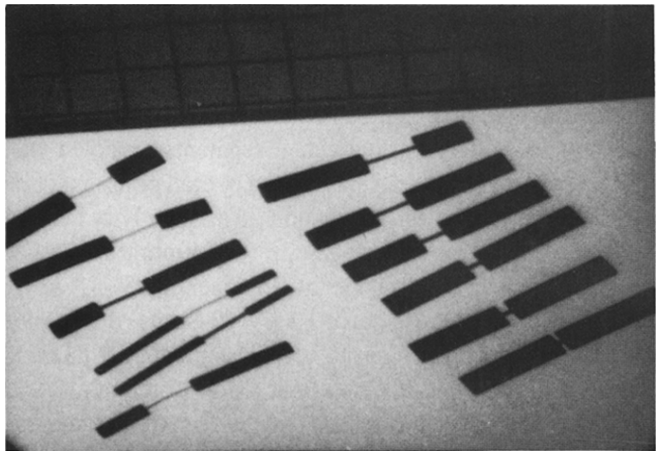

Figure 4. Radiographic image of the copper phantoms, each containing a complex obstruction of specific size and length.

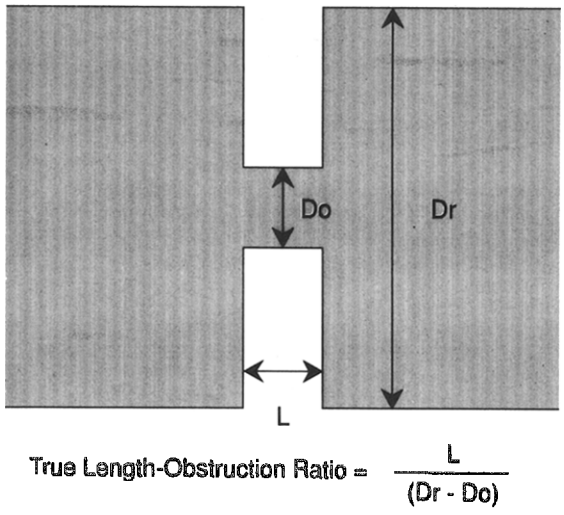

Figure 5. For each copper phantom, the true length (L)/obstruction ratio is defined as a variable describing the complexity of the lesion. The most complex lesions are characterized by small length/obstruction ratios. Do = obstruction diameter; Dr = reference diameter.

and filled with 100% contrast medium (Iopamiro) were acquired with the Philips digital angiographic image acquisition system DCI at an image intensifier mode of 7 in. (17.8 cm) and an X-ray tube voltage of 70 kV. The phantom was placed on top of a stack of 10 cm of plexiglass functioning as scatter medium. Each "vessel" segment was analyzed over a length of ~2 cm, resulting in a mean diameter and a standard deviation both expressed in millimeters. The precision per segment is defined by the standard deviation of the signed differences between each measured diameter in the diameter function and its corresponding mean value; this standard deviation is a measure for the irregularity of the detected contours. Accurate calibration was performed on the basis of a centimeter grid that was acquired simultaneously with the plexiglass phantom.

Copper phantoms. The second validation study was carried out with 12 copper phantoms with U-shaped obstructions of various lengths and diameters (Fig. 4). The size of the obstruction diameter was either 0.5 or 1.0 mm, whereas the diameter of the nonobstructed part of the phantom ranged from 2 to 5 mm. The obstruction length ranged from 1 to 10 mm. To assess the effectiveness of the gradient field transform in the detection of severe obstructions with short lengths, we introduced the "length/obstruction ratio" for each phantom. This value is defined by the true length of the obstruction divided by the difference between the true reference and obstruction diameters at the site of the minimal lumen diameter (Fig. 5). This measure is an adequate tool to describe the complexity of the type of lesions as observed in the copper phantoms. Its applicability to other types of complex lesions (dissections, thrombolytic obstructions) is more limited. For each phantom, the difference between measured and true obstruction diameters was calculated. The measured obstruction diameter was defined by the minimal value in the diameter function.

Coronary angiograms. In a third evaluation study 25 coronary segments were selected from 19 routinely acquired digital arteriograms. These segments were selected on the basis of the presence of irregularly shaped obstructions. Both algorithms were applied to each segment twice, and for each approach the obstruction diameter, the computer-defined or interpolated reference diameter, the length of the obstruction, the area of the atherosclerotic plaque and the stenotic flow reserve values were assessed. The plaque area is defined by the integrated area between the lumen and reconstructed reference contours between the obstruction boundaries (4–6). The stenotic flow reserve is a measure for the functional significance of an obstruction according to the principles described by Kirkeeide et al. (9,10). By calculating the differences between the first and second measurements, the intraobserver accuracy and precision values for all recorded variables can be established for both approaches. In addition, the differences between the two approaches can be assessed from all of the measurements.

Statistics. For the plexiglass phantom studies, each "vessel" segment analyzed was characterized by a mean diameter and a standard deviation value. The standard deviation value is a measure for the irregularity of the contours. To obtain an overall measure for the plexiglass phantom acquired under a certain imaging condition, the mean signed differences between the true vessel sizes and the measured diameters were averaged over all segments, providing an overall accuracy value. The reproducibility or precision was defined by the pooled standard deviation of the measurements.

For clinical material, the accuracy of a particular variable was defined by the mean signed differences of the first and second analyses over all 25 segments. The precision was defined by the standard deviation of these differences. The accuracy therefore represents the systematic error between repeated analyses and the precision the variability of these measurements as carried out by one observer (intraobserver

Table 1. Accuracy and Precision Values of the Gradient Field Transform and Minimum Cost Algorithm as Measured From the Plexiglass Phantoms

True Diameter (mm)	GFT (mm)		MCA (mm)	
	Accuracy	Precision	Accuracy	Precision
0.660	+0.102	0.133	+0.114	0.111
0.787	+0.057	0.132	+0.067	0.135
1.017	−0.013	0.113	+0.006	0.101
1.321	+0.073	0.121	+0.015	0.107
1.702	−0.048	0.122	−0.017	0.107
1.994	−0.037	0.121	+0.079	0.076
2.527	−0.028	0.111	−0.009	0.098
3.048	−0.030	0.099	−0.042	0.080
3.569	−0.069	0.101	−0.104	0.085
4.039	−0.015	0.092	−0.106	0.067
5.055	−0.044	0.105	−0.024	0.067
Overall	−0.004	0.114	−0.001	0.096

GFT = gradient field transform; MCA = minimum cost algorithm.

statistics). The Student *t* test was used to assess the statistical significance of mean differences, and the F test was used for differences in precision values.

Results

Plexiglass phantom studies. The results of the plexiglass phantom studies are presented in Table 1 and in Figure 6. Table 1 gives the average difference (accuracy) between the measured and true diameter and the standard deviation of this difference (precision) of both the gradient field transform and the minimum cost algorithm for each separate tube and includes the overall accuracy and precision (pooled standard deviation) values. The differences between the measured mean diameters and the true values for the individual vessel segments are clearly illustrated in Figure 6, according to the method of Bland and Altman (11).

The overall accuracy of both algorithms is comparable (−0.004 mm for the gradient field transform vs. −0.001 mm for the minimum cost algorithm, p = NS). A negative accuracy value means that the actual measurements slightly underestimated the true dimensions. From the standard deviation values of the individual segments a pooled standard deviation can be calculated. The overall precision of the minimum cost algorithm (0.096 mm) was slightly better than that of the gradient field transform (0.114 mm). This difference was statistically significant (F value >0.95).

Copper phantoms. Figure 7 (top) illustrates the performance of the minimum cost algorithm on a copper phantom with a reference diameter of 5 mm, an obstruction diameter of 1 mm and an obstruction length of 2 mm. The minimal lumen diameter was severely overestimated at 2.77 mm. In contrast, the gradient field transform (Fig. 7, bottom) measured an obstruction diameter of 1.02 mm. The results for the length/obstruction ratios are presented in Figure 8. The length/obstruction ratio is used to quantify the severity of the obstruction. The difference between the measured minimal lumen diameter and the true obstruction diameter is given along the vertical axis, and the true length/obstruction ratio is given along the horizontal axis. It is very obvious that the gradient field transform provides very reliable data over the whole range of ratios, whereas large overestimations in the measured obstruction diameter are found with the minimum cost algorithm for ratio values <1.2.

Coronary arteriograms. The intraobserver accuracy and precision values for the obstruction diameter, interpolated reference diameter, obstruction length, plaque area and stenotic flow reserve for the complex coronary obstructions are presented in Table 2 for both the gradient field transform and the minimum cost algorithm. In addition, data for the minimum cost algorithm for noncomplex lesions, as assessed from an earlier study, are shown (5). The accuracy values for all variables in complex or noncomplex lesions are all close to zero for both approaches and were not found to be statistically significantly different. This means that system-

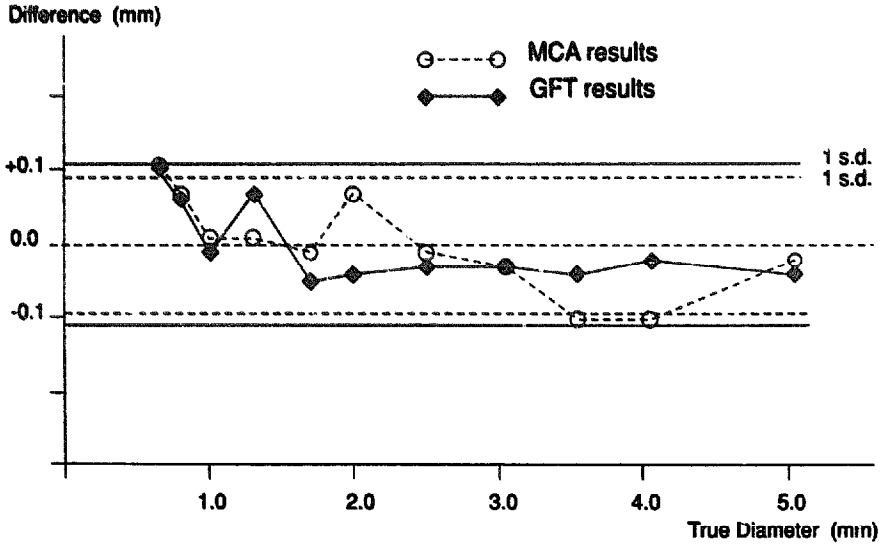

Figure 6. Signed differences between the averaged measured and true diameters of the plexiglass phantom given for the gradient field transform (GFT) and minimum cost algorithm (MCA) as a function of the true diameters of the vessel tubes. Horizontal lines represent precision values (pooled standard deviation [s.d.]). A negative difference corresponds to an underestimation, a positive difference to an overestimation of the measured sizes.

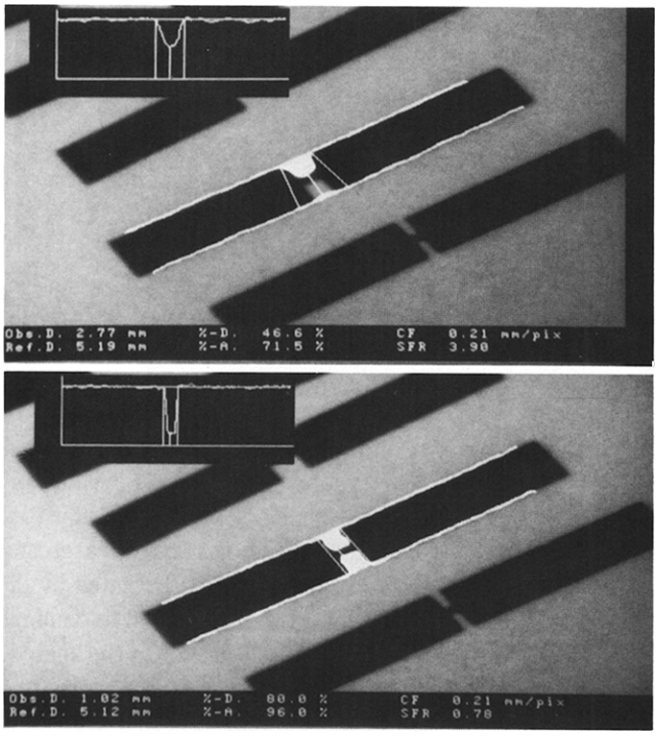

Figure 7. Copper phantom with 5-mm reference diameter (Ref.D.), 1-mm obstruction diameter (Obs.D.) and 2-mm obstruction length analyzed by the minimum cost algorithm (top) and gradient field transform (bottom). The minimum cost algorithm severely overestimated the obstruction diameter (2.77 mm), whereas the gradient field transform found a 1.02-mm obstruction diameter.

atic errors do not occur during repeated analysis with either of the approaches. On the other hand, the precision values for the different variables as assessed with the minimum cost algorithm in the complex lesions roughly double those for the noncomplex lesions. However, the precision of the gradient field transform in the complex lesions for the obstruction and reference diameters are of the same order of magnitude as the minimum cost algorithm for noncomplex lesions. This demonstrates the effectiveness of the gradient field transform in quantitative analysis of complex lesions. Unfortunately, we did not find a similar decrease in variability for the other variables of obstruction length and plaque area. On the other hand, the precision of the stenotic flow reserve, which chiefly depends on the ratio between obstruction and reference diameters, was found to be similar to the precision of the stenotic flow reserve in noncomplex lesions, as measured by the minimum cost algorithm.

In Table 3 the values obtained with the gradient field transform and the minimum cost algorithm for the complex lesions are compared; all analysis results, inclusive of the repeated analyses, are included, resulting in 50 measurements. On average, the gradient field transform finds smaller obstruction diameters than the minimum cost algorithm; the average difference equals 0.252 mm ($p < 0.0005$). On the other hand, no significant differences were found for the reference diameter, obstruction length and plaque area. Finally, stenotic flow reserve values were found to be significantly different (-0.721, $p < 0.0005$).

The processing time for the gradient field transform is much longer than that for the minimum cost algorithm for the same coronary segment (average 37 s vs. 9 s on a 80386 personal computer). This is mainly due to the more complicated way in which the edge strength is calculated and the fact that the gradient field transform requires linear interpolation in the zooming procedure instead of the pixel replication that is sufficient for the minimum cost algorithm.

Discussion

In this report a novel approach for the accurate assessment of coronary boundaries in digital arteriograms is presented and validated. The algorithm, the gradient field transform, was especially designed for the detection of the contours of complex lesions, with abruptly changing vessel dimensions. In practical terms this means that the new contour detection technique should be able to follow automatically the shape of obstructions of any complexity, even

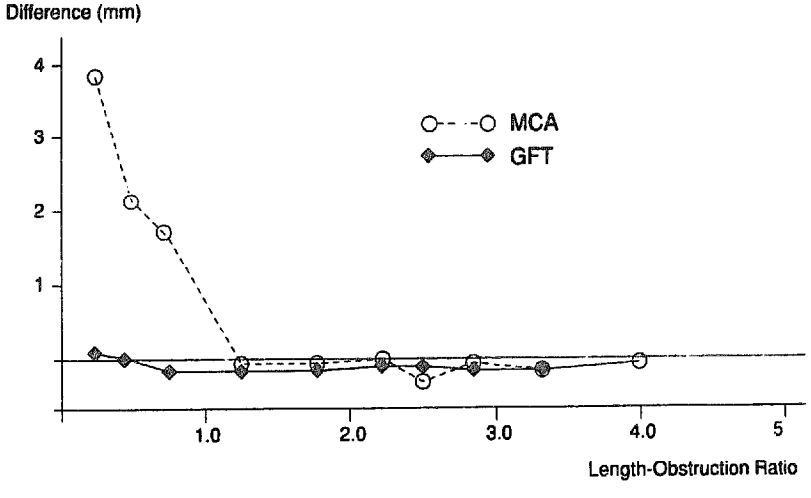

Figure 8. Differences between measured and true minimal obstruction diameters for the gradient field transform (GFT) and minimum cost algorithm (MCA) as a function of the length/obstruction ratio. The gradient field transform clearly provides accurate obstruction diameters over the entire range, whereas the minimum cost algorithm severely overestimated the obstruction diameters for length/obstruction ratios <1.2.

JACC Vol. 24, No. 1
July 1994:216–24

Table 2. Intraobserver Data for the Gradient Field Transform and Minimum Cost Algorithm for the Most Relevant Variables as Assessed From 25 Complex Coronary Artery Segments From Digital Arteriograms

Variable	GFT (n = 25)		MCA (n = 25)		Noncomplex Lesions, MCA (n = 39)	
	Accuracy	Precision	Accuracy	Precision	Accuracy	Precision
Obstruction diameter (mm)	−0.03	0.14	−0.03	0.20	0.03	0.10
Reference diameter (mm)	−0.04	0.12	0.00	0.21	0.03	0.13
Obstruction length (mm)	−0.31	2.61	0.36	2.01	0.36	1.22
Area of plaque (mm^2)	−0.31	2.37	0.03	2.83	0.22	1.29
Stenotic flow reserve	−0.06	0.39	−0.12	0.62	0.06	0.21

All differences were not found to be statistically significantly different. For comparison purposes, the minimum cost algorithm (MCA) accuracy and precision values for noncomplex lesions as assessed earlier (5) have been added. GFT = gradient field transform.

those with overhanging flaps and dissections, as are frequently found after a recanalization procedure.

Evaluation of plexiglass phantoms. The results from the studies using contrast-filled plexiglass phantoms indicate that the gradient field transform is comparable to the minimum cost algorithm when smooth vessel segments are analyzed. The irregularity of the edges along these smooth vessel segments as expressed by the standard deviation values was found to be slightly higher for the gradient field transform (0.114 mm) compared with the minimum cost algorithm (0.096 mm), and the accuracy was comparable (−0.004 vs. −0.001 mm, respectively). The slightly larger precision value results from the much larger number of possible contours for the gradient field transform than for the minimum cost algorithm. Some artifacts, caused by noise, could not be found by the minimum cost algorithm because of the restrictions imposed on that algorithm; however, these were found by the gradient field transform. Figure 6 makes clear that overestimations in vessel sizes <1.2 to 1.3 mm are limited to 0.1 mm. This demonstrates that the correction procedure for the limited resolution of the X-ray system performs appropriately.

The propensity of the gradient field transform to pick up noise is undesirable when smooth, healthy vessel segments are analyzed. It is clear from the data in Table 1 and the example in Figure 3 that the vessel contours that are detected by the gradient field transform exhibit a greater irregularity or roughness than the contours detected by the minimum cost algorithm. It is therefore our goal to combine the two algorithms in the final implementation of the analytic software package. In this new approach, any analysis of a coronary segment starts with the minimum cost algorithm. Only those parts of the coronary segments that are labeled as an obstruction by the minimum cost algorithm will be reanalyzed by the gradient field transform. This scenario can be fully automated, so that no additional user interaction is required.

Table 3. Intratechnique Accuracy and Precision Values as Assessed From All Measurements Obtained With the Gradient Field Transform and Minimum Cost Algorithm

Variable	Average Difference GFT − MCA (n = 50)	SD of Differences GFT − MCA (n = 50)
Obstruction diameter (mm)	−0.252 (p < 0.0005)	0.259
Reference diameter (mm)	−0.013 (p = NS)	0.232
Obstruction length (mm)	−0.280 (p = NS)	2.791
Area of plaque (mm^2)	0.47 (p = NS)	3.722
Stenotic flow reserve	−0.721 (p < 0.0005)	0.743

Abbreviations as in Table 1.

Copper phantoms. On review of the results of the copper phantom studies, it is evident that the gradient field transform performed much better than the minimum cost algorithm for obstructions with a short length (length/obstruction ratio <1.2). In this evaluation the true length of the obstruction was used instead of the length as it is calculated by the program. For very short obstructions, the program severely overestimated the length of the obstruction. The current version of the algorithm for the definition of the length of an obstruction determines the distance between the first diameter positions on either side of the minimal lumen diameter for which the arterial diameter exceeds the corresponding reference diameter or when a local maximum is reached in the arterial diameter and its value is >90% of the corresponding reference diameter. To limit measurement variability, some smoothing is applied during calculation of the obstruction length. Because of the sharp transitions in values for the arterial diameter this algorithm is therefore inadequate to properly measure the true length of the obstruction. Further research will be necessary to solve this problem.

For length/obstruction ratios >1.2, both algorithms performed comparably, both underestimating the actual minimal lumen diameter (−0.08 mm for the minimum cost algorithm; −0.11 mm for the gradient field transform). This underestimation is caused by the fact that for a particular obstruction of sufficient extent a number of obstruction diameters are assessed, of which only the smallest value is taken to represent the actual minimal lumen diameter. Be-

cause of noise, the measured obstruction diameter will be smaller than the actual obstruction diameter.

Coronary arteriograms. The third part of the evaluation performed on routinely acquired digital coronary arteriograms allowed us to study two kinds of accuracy and precision values: those obtained from intraobserver comparisons and an intratechnique comparison. The intraobserver data were presented in Table 2. The various accuracy values, which define the average or systematic overestimation or underestimation of the measurements, were all close to zero for both algorithms, and the differences were not statistically significant.

The majority of the coronary artery segments selected had small obstruction diameters or an irregular shape. For 16 of the 25 segments the gradient field transform algorithm measured an obstruction diameter <1 mm, with reference diameters >2 mm, whereas for 7 of these submillimeter obstructions a reference value >3 mm was found.

For this set of images, the intraobserver precision of the obstruction diameter for the gradient field transform algorithm (0.14 mm) was significantly better than that for the minimum cost algorithm (0.20 mm, F test p value < 0.05). This is due to the fact that the gradient field transform is influenced less by the actual position of the initial pathline model. When comparing these data with those from earlier published data (3) on the minimum cost algorithm for noncomplex lesions (Table 2), it becomes apparent that the minimum cost algorithm variability increases sharply for complex lesions, whereas the gradient field transform precision remains on the same order of magnitude as the minimum cost algorithm precision for noncomplex lesions. This demonstrates the effectiveness of the gradient field transform in the analysis of complex lesions. The same phenomenon for the precision values was found for the interpolated reference diameter values and the stenotic flow reserve. The precision of the stenotic flow reserve mainly depends on the precision by which both the obstruction diameter and the corresponding reference diameter can be measured. The improvement in the precision in obstruction and reference diameters by the gradient field transform results in an improvement in the precision of the stenotic flow reserve for the gradient field transform compared with the minimum cost algorithm. It is not clear why the intraobserver variabilities in obstruction length and plaque area were hardly influenced by the algorithm.

Finally, in Table 3 the intratechnique accuracy and precision values were presented for the complex lesions. Because the gradient field transform can follow more severe and more abruptly changing vessel dimensions, we expected the gradient field transform obstruction diameters to be smaller than the corresponding minimum cost algorithm obstruction diameters. This was clearly demonstrated by the data, with an average signed difference of 0.252 mm ($p < 0.0005$).

This particular finding may have a very important impact on the calculation of restenosis rates, depending on the actual measurement of the minimal lumen diameter in restenosis trials. If current practice in core laboratories is to manually edit those severe complex lesions toward smaller obstruction diameters, as demonstrated in this study, little effect is to be expected. However, in our opinion common practice has been to limit manual editing as much as possible, particularly at obstructions, so that the high precision in the measurements is not sacrificed. A 0.72-mm change from postangioplasty to follow-up has been used as one of several restenosis criteria (12); this criterion has been defined by two standard deviations of the long-term variability, as measured with CAAS (1). Our new results demonstrate an urgent need for a medium- or long-term variability study, using the new gradient field transform, to establish a new absolute criterion. The interpolated reference diameters were found to be similar on average for both algorithms. This can be explained by the fact that the calculation of the reference diameter function is based predominantly on diameter values outside the obstruction area (i.e., in the relatively smooth, straight parts of the vessels). In this case the data showed a nonsignificant difference of only 0.01 mm.

The differences in stenotic flow reserve values as measured by both algorithms were significant. The ability of the gradient field transform to measure sharper obstructions resulted in a significantly lower stenotic flow reserve (average difference −0.721, $p < 0.0005$). Precision was also better with the gradient field transform (0.39 vs. 0.62 for the minimum cost algorithm).

Conclusions. This validation study clearly demonstrated the effectiveness of the gradient field transform in accurately delineating the contours of complex lesions. This was also evident from visual inspection of the contours detected by either of the algorithms. However, we believe that both the gradient field transform and the minimum cost algorithm will find their own applications in quantitative coronary arteriography. The minimum cost algorithm performs best in relatively smooth segments, whereas the gradient field transform is superior at irregular lesions. Therefore, the final implementation of a new coronary analytical software package will incorporate both approaches.

References

1. Reiber JHC, Serruys PW, Kooyman CJ, et al. Assessment of short-, medium- and long-term variations in arterial dimensions from computer-assisted quantification of coronary cineangiograms. Circulation 1985;71: 280–8.
2. Reiber JHC, Serruys PW, editors. Quantitative Coronary Arteriography. Dordrecht: Kluwer Academic Publishers, 1991:327.
3. Reiber JHC, Serruys PW. Quantitative coronary arteriography. In: Marcus ML, Skorton DJ, Schelbert HR, Wolf GL, editors. Cardiac Imaging. Philadelphia: Saunders, 1991:211–81.
4. Reiber JHC, Zwet PMJ van der, Land CD von, et al. Quantitative coronary arteriography: equipment and technical requirements. In: Reiber JHC, Serruys PW, editors. Advances in Quantitative Coronary Arteriography. Dordrecht: Kluwer Academic Publishers, 1992:75–111.
5. Reiber JHC, Zwet PMJ van der, Koning G, et al. Accuracy and precision of quantitative digital coronary arteriography; observer-, as well as

short- and medium-term variabilities. Cathet Cardiovasc Diagn 1993;28: 187–98.

6. Zwet PMJ van der, Land CD von, Loois G, Gerbrands JJ, Reiber JHC. An on-line system for the quantitative analysis of coronary arterial segments. Comput Cardiol 1990:157–61.
7. Gerbrands JJ. Segmentation of noisy images [dissertation]. Delft, The Netherlands: Delft University of Technology, 1988:136.
8. Dijkstra EW. A note on two problems in connection with graphs. Numerische Mathematik 1959;1:269–72.
9. Kirkeeide RL, Gould KL, Parsel L. Assessment of coronary stenoses by myocardial perfusion imaging during pharmacologic coronary vasodilation VII. Validation of coronary flow reserve as a single integrated functional measure of stenosis severity reflecting all its geometric dimensions. J Am Coll Cardiol 1986;7:103–13.
10. Kirkeeide RL. Coronary obstructions, morphology and physiologic significance. In Ref. 2:229–44.
11. Bland JM, Altman DG. Statistical methods for assessing agreement between two methods of clinical treatment. Lancet 1986;2:307–10.
12. Serruys PW, Hermans WRM, Rensing BJ, de Feyter PJ. Pharmacological prevention of restenosis after percutaneous transluminal coronary angioplasty (PTCA): overview and methodological considerations. In: Reiber JHC, Serruys PW, editors. Advances in Quantitative Coronary Arteriography. Dordrecht: Kluwer Academic Publishers, 1993:329–50.